Available online at www.sciencedirect.com
SCIENCE DIRECT®
Journal of Solid State Chemistry 177 (2004) 4616–4625
JOURNAL OF SOLID STATE CHEMISTRY
www.elsevier.com/locate/jssc

Structural study of lanthanum nickelate thin films deposited on different single crystal substrates

Vincent Faucheux, Stéphane Pignard, Marc Audier*

LMGP-ENSPG-INPG, INPG-CNRS, UMR 5628, BP 46, FR-38402 Saint Martin d'Hères, Cedex, France

Received 28 July 2004; received in revised form 5 October 2004; accepted 13 October 2004
Available online 13 November 2004

Abstract

Fabrications of $La_2NiO_{4+\delta}$ thin film layers by liquid-injection metalorganic chemical vapor deposition were tried on different single crystals substrates: (001)Si, (001)MgO, (001)$LaAlO_3$ and (001)$SrTiO_3$. As results of structural characterizations, polycrystalline dendritic layers of $La_2NiO_{4+\delta}$ tetragonal (or orthorhombic) phase were observed on (001)Si substrates while layers of a perovskite-like cubic structure were observed on the other single crystal substrates. From a high-resolution TEM study of a layer deposited on (001)MgO, such a perovskite-like cubic structure exhibits many planar structural faults likely similar to planes of oxygen vacancies of the $La_2NiO_{4+\delta}$ orthorhombic structure. A thin intermediate epitaxial layer of NiO phase was also identified. Using a X-ray texture diffractometer, the layer structure on (001)MgO, (001)$LaAlO_3$ and (001)$SrTiO_3$ was confirmed to be of cubic structure with ⟨100⟩ axes parallel to those of the substrate. The T dependence of the resistivity of a layer deposited on (001)MgO substrate was found to be of a semi-conducting behavior.

Keywords: Ruddlesden–Popper oxide; Metalorganic chemical vapor deposition; Transmission electron microscopy; X-ray diffraction

1. Introduction

$La_2NiO_{4+\delta}$ is a K_2NiF_4-type compound and has widely been studied as it is isostructural with the high T_c superconducting compounds $La_2CuO_{4+\delta}$ discovered in 1986 [1]. Like $La_2CuO_{4+\delta}$, $La_2NiO_{4+\delta}$ exhibits a wide range of oxygen stoechiometry which has been attributed to the presence of intergrown phases or deviation in the metal–atom ratio [2]. Most of the studies concerned magnetic, ionic transport and structural properties of $La_2NiO_{4+\delta}$ single crystals or ceramic powders (e.g. Refs. [3–8]). Besides fundamental aspects, several potential applications of the $La_2NiO_{4+\delta}$ compound are often mentioned in these studies. For instance, the preparation of more efficient cathodes for solid oxide fuel cells working at intermediate temperature (about 700 °C) or the preparation of membranes for oxygen purification or partial oxidation of alcanes. Among the number of ionic conductor oxides, it is mentioned that due to its large oxygen excess δ (i.e. as large as 0.18 [5,9,10]), the $La_2NiO_{4+\delta}$ oxide could exhibit interesting capacities toward both oxygen reduction and efficient O^{2-} diffusion [8,11,12]. For this reason, we were interested to examine whether this compound might be prepared as thin film layers using a technique of metalorganic chemical vapor deposition (MOCVD) which, for industrial applications, offer the possibility to grow layers on large substrate surfaces at a low-cost. To our knowledge, only one study has been carried out on an epitaxial growth of $La_{2-x}Sr_xNiO_4$ thin films with $1.5 \geqslant x \geqslant 0.5$ [13] but synthesized by pulsed-laser deposition (PLD) utilizing a KrF excimer laser (248 nm).

In this paper, we investigate the structural characteristics and some physical properties of lanthanum nickel

*Corresponding author. Fax: +33 4 76 82 63 94.
E-mail address: Marc.Audier@inpg.fr (M. Audier).

0022-4596/$ - see front matter © 2004 Elsevier Inc. All rights reserved.
doi:10.1016/j.jssc.2004.10.016

oxide thin films obtained by MOCVD. The study is carried out for films grown on different single crystalline substrates in relation to a further study of anisotropic physical properties which could be induced by an epitaxial growth. Depending on the substrate used, Si or a metallic oxide, the thin film microstructures and structures are shown to be different. They are either dendritic with a structure of $La_2NiO_{4+\delta}$ phase or columnar with a perovskite-like cubic structure exhibiting many plane structural faults. Magnetic and transport properties are also reported for films deposited on (001)$LaAlO_3$ and (001)MgO substrates.

2. Experimental

Lanthanum nickelate oxide layers in a thickness range of 400–900 nm were deposited on different single crystal substrates by pulsed liquid-injection MOCVD. A detailed description of this experimental technique with general conditions for thin film layer fabrications have been presented in Ref. [14]. Let us recall however, that particular characteristics of this MOCVD technique are that a sequential injection of micro-amounts of a liquid solution of solid precursors diluted in a solvent is realized using an injector of the same type as those used for the fuel injection in thermal motors [15]. These droplets of a few milliliters are injected in a cold zone on a moving tape where, at a working pressure of a few hundreds Pa, the solvent is immediately evaporated and eliminated in situ. The precise micro-amount of solid precursor lying on the moving belt is mechanically carried into an evaporation zone (typically heated between 200 and 300 °C) where the precursor vapors are produced. These vapors are then carried into the reaction zone where a classical CVD reaction occurs on a substrate. The flow rate of precursors in the evaporator depends on an electrical pulse width, the injection frequency, the viscosity of the solution of precursors and on the pressure difference between a vessel containing this solution (pressurized at about 3×10^5 Pa of argon) and the evaporation chamber.

Lanthanum nickelate oxide compounds were obtained from a solution of metalorganic precursors $La(thd)_3$ and $Ni(thd)_2$ dissolved in 1,2-dimethoxyethane solvent at a total concentration of 0.02 mol L^{-1}. As in this case, the ratio of the precursors in solution is different from the composition of the films because each precursor has a different decomposition and deposition yield, we have firstly determined the linear relationship between these ratios. As a result, it was found that $(La/Ni)_{layer} = 0.816(La/Ni)_{solution}$ for $3 \geqslant (La/Ni)_{solution} \geqslant 0.5$. The overall $(La/Ni)_{layer}$ ratios were systematically determined by X-ray wavelength dispersive spectroscopy (XWDS) on a CAMECA microprobe. However, from X-ray diffraction analyses it was found that a precipitation of La_2O_3 phase occurs for $(La/Ni)_{solution} \geqslant 2.33$. Thus in order to avoid the formation of La_2O_3 phase, we have used solutions containing a same precursor ratio of 2.33 for all the layer growth experiments on the different single crystal substrates. The resulting La/Ni ratios in fabricated layers were therefore all of 1.9 instead of 2 as it should be required for a formation of $La_2NiO_{4+\delta}$ compound.

Metalorganic vapors were transported in a carrier gas flux of 10 $cm^3 s^{-1}$, constituted of O_2(33.33%) and Ar (66.66%) under a total pressure of 660 Pa. The deposition temperature was 650 °C and the film growth rate was about 1.2 μm h^{-1}. Samples were cooled down to room temperature under the O_2–Ar gas flux at a rate of 2 °C min^{-1}.

Both the cell parameters and thermal expansion coefficients of the four single crystal substrates used are compared to those of the $La_2NiO_{4+\delta}$ compound in Table 1. For the $La_2NiO_{4+\delta}$ compound, we have only indicated the cell parameters of an orthorhombic structure because the cell parameters of other structural forms of $La_2NiO_{4+\delta}$ compounds are very close of these values. From a comparison of the a and c cell parameter values of this $La_2NiO_{4+\delta}$ compound with those of the different single crystal substrates, it appears that an epitaxial growth on a (001)Si substrate could be expected with a small cell misfit of the order of 1.5% for an epitaxy corresponding to $(010)_L//(001)_S$ and $[100]_L//[100]_S$ where the subscripts L and S stand for layer and substrate, respectively. In the case of both (001)$SrTiO_3$ and (001)$LaAlO_3$ substrates, the expected epitaxy could be $(010)_L//(001)_S$ and $[101]_L//[100]_S$ with a misfit of reticular distances of the order of 1–2% while it would be much more important for a (001)MgO substrate (i.e. about 8%). Besides, as an eventual layer cracking is directly related to the difference of thermal expansion coefficients (TEC), a comparison of TEC values as reported in Table 1 indicate that this of $La_2NiO_{4+\delta}$ is similar to those of $LaAlO_3$ and MgO substrates but not with this of silicon. Such a comparison cannot be made in the case of a $SrTiO_3$ substrate because of a large discrepancy between TEC values reported in the literature.

The structures of the deposited layers were studied by X-ray diffraction using $\theta/2\theta$ and texture diffractometers and, only for layers deposited on (001)Si and (001)MgO substrates, by transmission electron microscopy (TEM). For TEM investigations, the prepared sample were either cross-section thin foil specimens obtained by ion milling or small layer fragments, obtained by scratching the layer surface with a diamond tip, which were deposited on copper grids coated with a carbon film. Variations of La/Ni ratios through layer thickness were also qualitatively analyzed on cross-section specimens by XEDS–TEM for the layer deposited on the (001)MgO substrate.

Table 1
Crystal properties: cell parameters and TEC

Material	Crystal lattice	Unit cell parameters	Average TEC ($\times 10^{-6}$ K)	Refs.
$La_2NiO_{4+\delta}$	orthorhombic or tetragonal	$a = 5.4618$ Å, $b = 12.561$ Å, $c = 5.4967$ Å	13.7	[16]
Si	cubic ($Fd\bar{3}m$)	$a = 5.42$ Å	2.6	[17,19,20]
$SrTiO_3$	cubic ($Pm\bar{3}m$)	$a = 3.905$ Å	from 11 up to 32.3	[17,18]
$LaAlO_3$	pseudocubic	$a = 3.79$ Å	10.0	[17,19,20]
MgO	cubic ($Fm\bar{3}m$)	$a = 4.21$ Å	13.47	[17,19,20]

3. Results

Only the structure of layers deposited on the (001)Si wafer, was found by electron diffraction to be in agreement with that of a $La_2NiO_{4+\delta}$ compound (see after). However, electron diffraction is not enough precise for accurate comparisons of our experimental data with different crystallographic data reported in the literature. Let us recall that the structural states of $La_2NiO_{4+\delta}$ compounds depend on both the temperature and the oxygen excess δ. The reported structures are either tetragonal with different spacegroups ($I4/mmm$, $P4_2/ncm$) or orthorhombic also with different spacegroups ($Fmmm$, $Bmab$ (or $Cmca$ in the standard notation)). Between these structural forms there are only slight changes of cell parameter values and atomic positions. For instance, the stoechiometric La_2NiO_4 compound is orthorhombic ($Cmca$, $a = 5.4499$ Å, $b = 12.5118$ Å, $c = 5.5275$ Å) at room temperature and transforms into a tetragonal structure $I4/mmm$ at $T \cong 770$ K [9].

As represented in Fig. 1(a), the $La_2NiO_{4+\delta}$ orthorhombic structure is constituted of sheets of corner-sharing NiO_6 octahedra. These octahedra are slightly tilted with respect to each other and the La ions are positioned in the layer formed by the apical oxygens. There are oxygen vacancies in planes at $y = \frac{1}{4}$ and $y = \frac{3}{4}$. So far, the maximum oxygen excess δ reported in the literature is 0.18 [16], which means that a maximum of 9% of these vacancy sites can be occupied by oxygen atoms. Besides, the slight tilting of NiO_6 octahedra with respect to the **b**-axis would result of a slight size increase of the oxygen tetrahedron formed by apical oxygens of NiO_6 octahedra and surrounding each vacancy site occupied by an oxygen atom (Fig. 1(b)). These structural changes would therefore be at the origin of different crystal structures reported in the literature. However, interesting results reported by Sayagués et al. [4] were to show that modulated structures of $La_2NiO_{4+\delta}$ can as well be formed for accommodating the oxygen excess. In this case, structures commensurately modulated along the **a**- or **c**-axes of the orthorhombic structure were observed by high-resolution TEM.

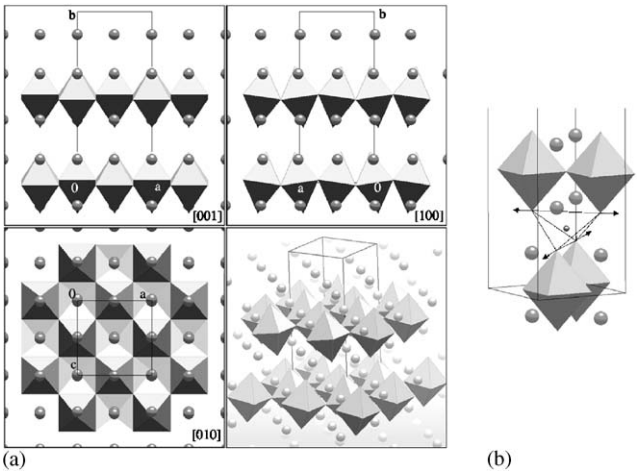

Fig. 1. (a) Atomic structure of the orthorhombic $La_2NiO_{4+\delta}$ compound (from crystallographic data presented in Ref. [9]: space-group $Cmca$, $a = 5.4618$ Å, $b = 12.561$ Å, $c = 5.4967$ Å); (b) oxygen vacancy surrounded by oxygen atoms situated at the vertices of a tetrahedron and which moved along the arrows when the vacancy site is occupied.

3.1. Structure and microstructure of $La_2NiO_{4+\delta}$ layers on (001)Si substrate

From TEM observations, the cross-sectional microstructure of layers deposited on (001)Si substrates appeared to be dendritic (Fig. 2(a)). The layer is not dense as dendrites appear to be separated from each other exhibiting a feather-like striated contrast. The structure of the $La_2NiO_{4+\delta}$ phase was verified from an indexing of electron diffraction patterns corresponding to a selected area on a layer fragment obtained by scratching the layer surface with a diamond tip (Fig. 2(b) and (c)). This fragment exhibits two domains with dendrite axes either parallel or tilted with respect to the direction of the incident electron beam. On the corresponding electron diffraction pattern, the positions

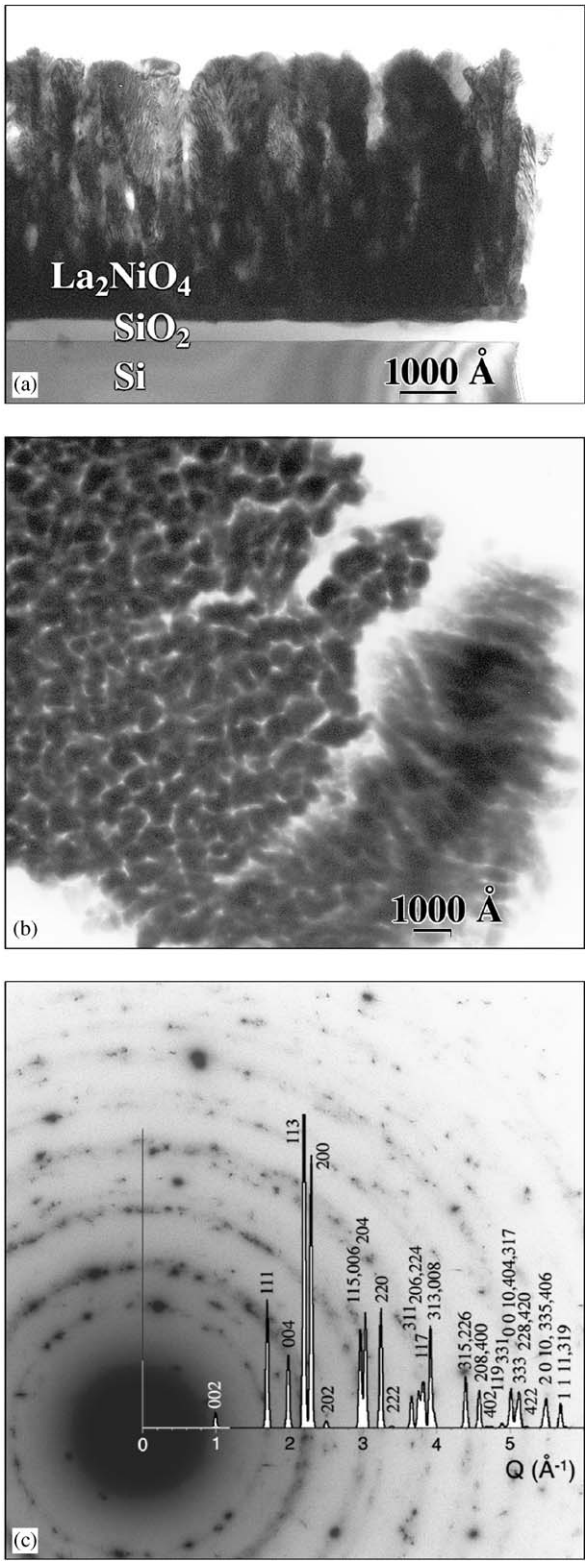

Fig. 2. (a) TEM cross-section images of a $La_2NiO_{4+\delta}$ layer, which was deposited on (001)Si wafer; (b) Bright field TEM image of a layer fragment and (c) corresponding electron diffraction pattern of a $La_2NiO_{4+\delta}$. The indexing of the diffraction pattern is made from a comparison with the simulated powder X-ray diffraction spectrum of the $La_2NiO_{4.18}$ tetragonal structure ($a = 5.46690$ Å, $c = 12.67804$ Å, space group $F4/mmm$), (after Ref. [9] for the crystallographic data).

and relative intensities of the dotted rings of reflections were found to be in accordance with the simulated powder diagram of a $La_2NiO_{4+\delta}$ tetragonal structure ($a = 5.46690$ Å, $c = 12.67804$ Å, space group $F4/mmm$) for which $\delta = 0.18$. However, as a reasonable good agreement was as well found for a powder diagram simulation based on other crystallographic data of a $La_2NiO_{4+\delta}$ orthorhombic structure, we cannot assert that this structures is actually tetragonal.

3.2. Structure of lanthanum nickelate oxide layers observed on (001)MgO, (001)$LaAlO_3$ and (001)$SrTiO_3$ single crystal substrates

Lanthanum nickelate oxide layers were deposited on these single crystal substrates in the same experimental conditions as those used for deposition on (001)Si wafer. By X-ray diffraction on a $\theta/2\theta$ diffractometer, just a few reflections were observed (Fig. 3). They correspond to diffracting vectors normal to the (001) substrate planes. Each $\theta/2\theta$ spectrum exhibits an intense 002 reflection due to the substrate and also very intense reflection at about 47° which could correspond to the 220 reflection of the tetragonal $La_2NiO_{4+\delta}$ structure ($a = 5.46690$ Å, $c = 12.67804$ Å, space group $F4/mmm$). However, from a comparison with the other reflection positions, it appears that the weak reflection observed at $2\theta = 23.2°$ does not correspond to the 111 reflection of this tetragonal structure. We have verified that it does not either correspond to reflections of other structural forms of $La_2NiO_{4+\delta}$ compounds.

Therefore, these layers appear to be, at least, strongly textured but one cannot conclude about their actual structure. Assuming that weak reflections might result of the presence of foreign phase then the following crystallographic orientation relationship between layer and substrate could be considered:

$$(110)_L//(001)_S.$$

However, this does not correspond to the expected epitaxy for a $La_2NiO_{4+\delta}$ tetragonal structure ($a = 5.46690$ Å, $c = 12.67804$ Å, space group $F4/mmm$), i.e. $(001)_L//(001)_S$ and $[110]_L//[100]_S$.

As whatever the substrate used, the X-ray diffraction reflections of layers remain similar, we have performed TEM investigations only on the layer deposited on the (001)MgO substrate in order to identify the film structure and eventually the presence of foreign phases.

3.2.1. TEM observations of the lanthanum nickelate oxide layer deposited on (001)MgO substrate

TEM observations were carried out on two cross-sections thin foil specimens, cut along both (100) and (110) planes of the MgO substrate. From the bright field image shown in Fig. 4(a), the microstructure of the layer appears to be columnar (and not dendritic as previously

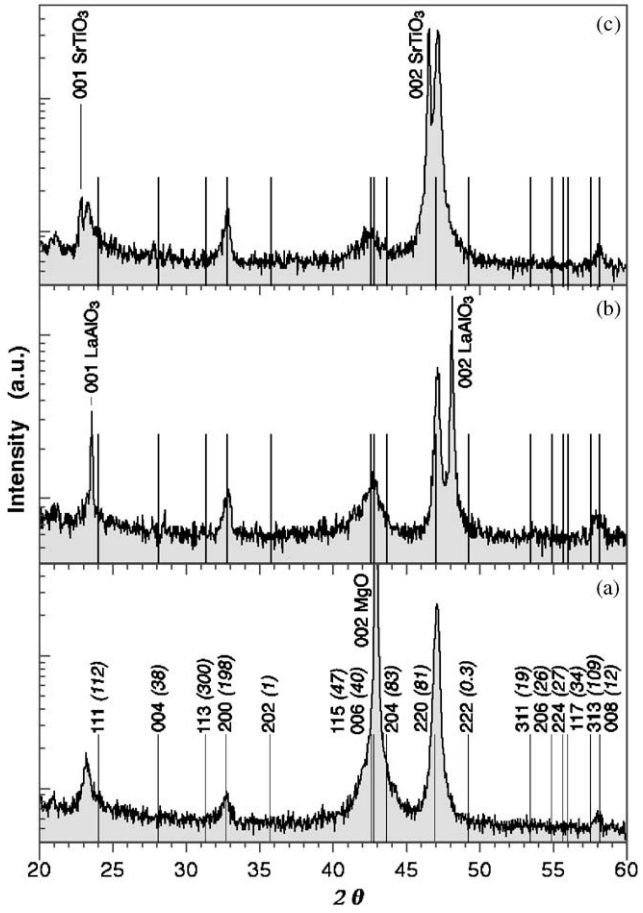

Fig. 3. $\theta/2\theta$ scans related to lanthanum nickelate oxide layers deposited on (a) (001)MgO, (b) (001)$SrTiO_3$ and (c) (001)$LaAlO_3$ substrates. For each spectrum, the main reflection observed could correspond to the 220 reflection of the $La_2NiO_{4+\delta}$ tetragonal structure ($a = 5.46690$ Å, $c = 12.67804$ Å, space group $F4/mmm$). (The hkl reflection positions of this structure are indicated with, in parenthesis, their relative intensities.) A foreign phase might be assumed since the weak reflection at $2\theta = 22.2^\circ$ is not in accordance with those of the $La_2NiO_{4+\delta}$ tetragonal structure.

observed for a layer on (001)Si substrate). There is an intermediate layer of about 4 nm thickness at the level of the layer–MgO interface (Fig. 4(b)) that we shall identified after. The selected area electron diffraction pattern (c) is related to part of the layer–MgO interface of the bright field image (a). In this case, the MgO substrate (of NaCl-type structure) is observed along a [110] zone axis from the indexing of its *fcc* reflections, indicated in the lower left part of the pattern. The

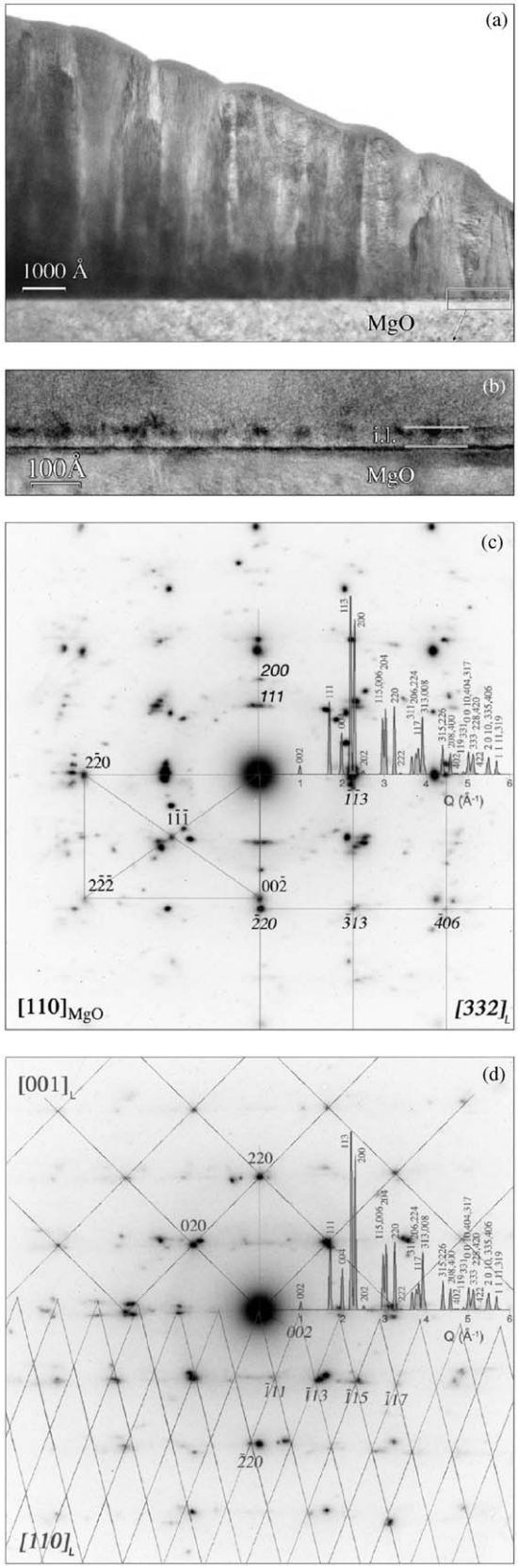

Fig. 4. (a) Bright field image of a cross-section of the lanthanum nickelate oxide layer deposited on a (001)MgO substrate and (b) enlargement of the interface showing the intermediate layer (i.l.); (c) corresponding electron diffraction pattern related to part of the layer–MgO interface and where the MgO substrate is oriented along a [110] zone axis; (d) diffraction pattern of a layer cross-section related to a [100] zone axis of orientation of the MgO substrate.

second diffraction pattern (d) is only related to a selected area of the layer but for the MgO substrate oriented along a [100] zone axis. For comparisons and scaling, a simulation of the powder X-ray diffraction spectrum of the $La_2NiO_{4+\delta}$ tetragonal structure is superimposed on each pattern. Both patterns exhibit well-defined periodic arrays of reflections and lines of diffuse scattering modulated in intensity. These lines were observed to be on either sides of a plane parallel to the layer–(001)MgO interface, within an angular range of about $\pm 7.5^\circ$. Among the reflections observed on the second pattern (d), a nearly square periodic array of reflections can easily be defined and indexed as a [001] zone axis of the $La_2NiO_{4+\delta}$ tetragonal structure and with a diffracting vector Q_{220} normal (or almost normal) to the$(001)_{MgO}$ substrate plane (i.e. in agreement with the previous X-ray diffraction results). As both patterns are related between them by a 45° rotation around this diffracting vector, one finds that a rectangular periodic array of reflections of zone axis equivalent to [332] for the $La_2NiO_{4+\delta}$ tetragonal structure could correspond to this rotation. However, a distortion of the $La_2NiO_{4+\delta}$ tetragonal structure should be considered in this case because the calculated angle between both these zone axes is of 42.45° instead of 45° corresponding to the angle between both [110] and [100] zone axes of the cubic MgO substrate. Besides, it can be noticed that the reflections observed on the pattern (c) do not exactly correspond to those of the simulated powder pattern, in particular the reflection of second-order 226. As a matter of fact, we have verified that both these arrays of reflections could as well be indexed as the [100] and [110] zone axes of a perovskite-like cubic structure of cell parameter 3.87 Å and with its $\langle 100 \rangle$ directions parallel to those of the MgO substrate structure. The existence of a structure close to this of the $La_2NiO_{4+\delta}$ tetragonal structure cannot, however, be discarded as a number of plane structural faults must be considered from the observed lines of diffuse scattering. Such lines can partly be indexed on the pattern (d) by considering the [110] zone axis of the $La_2NiO_{4+\delta}$ tetragonal structure where it appears that some intensity modulations are close to the reflection positions of this structure. Therefore, plane structural faults derived from the $La_2NiO_{4+\delta}$ tetragonal structure has to be considered as being perpendicular either to [100] or [010] directions of the MgO substrate.

In summary, the indexing of these electron diffraction patterns indicates that the average layer structure would be rather a simple perovskite-like cubic structure but with plane structural faults typical of structural features of the $La_2NiO_{4+\delta}$ structure. From the atomic structure of this phase shown in Fig. 1, such a structural faults could correspond to the planes of oxygen vacancies at $y = \frac{1}{4}$ and $\frac{3}{4}$. This interpretation can be confirmed from an analysis of a high-resolution image of the layer cross-section related to a [100] zone axis of orientation of the MgO substrate (Fig. 5). The Fourier transform of the high-resolution image, shown in inset of Fig. 5(a), is constituted of a square lattice of reflections with horizontal lines of diffuse scattering similar to what was observed on the electron diffraction (d) of Fig. 4. The trace of the layer–MgO interface with respect to this Fourier transform is, as for the electron diffraction

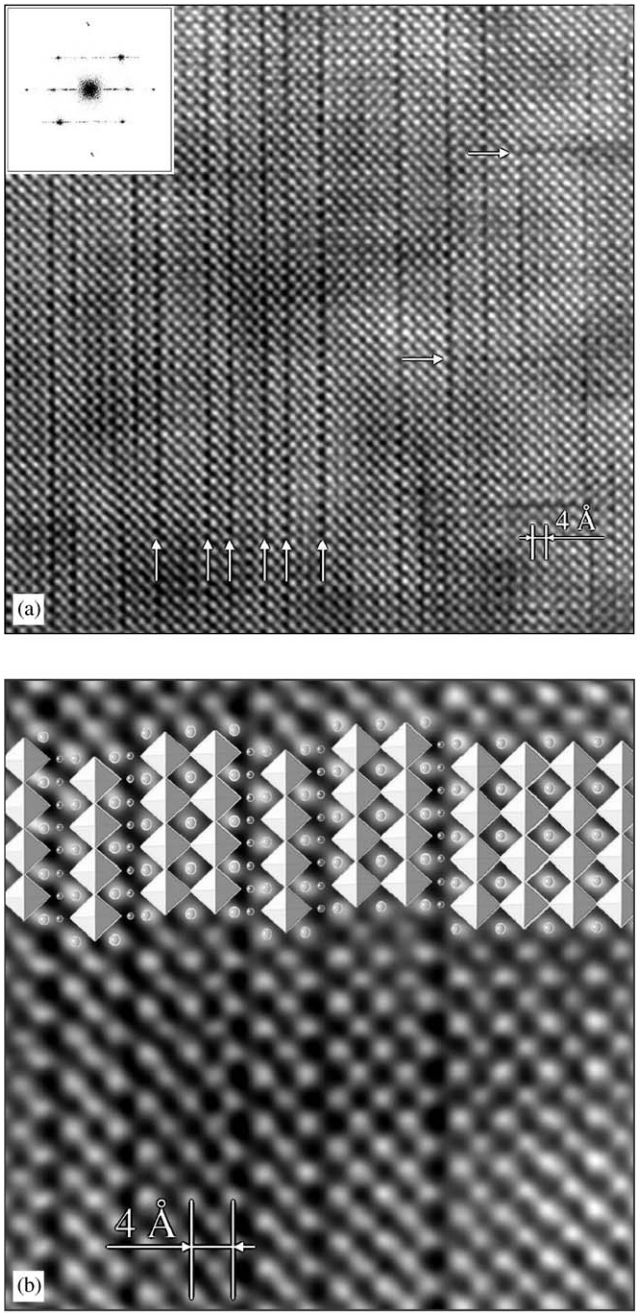

Fig. 5. (a) High-resolution image of the layer cross-section related to a [100] zone axis of orientation of the MgO substrate. In inset, the Fourier transform of the image appears to be similar of the electron diffraction pattern shown in (c). (b) Interpretation of the trace of the plane structural faults as planes of oxygen vacancies similar to those observed in the $La_2NiO_{4+\delta}$ orthorhombic structure shown in Fig. 1.

pattern, nearly horizontal. Thus, looking at the corresponding high-resolution image it can be deduced that the lines of diffuse scattering result of the vertical traces of plane structural faults (indicated by arrows) and that there are domains of pseudo square structure in between these traces. Let us notice that there are also a few horizontal traces of plane structural faults but their number is not sufficient to give rise to observable vertical lines of diffuse scattering.

Such a high-resolution image can directly be compared to a structural model derived from the atomic structure of the $La_2NiO_{4+\delta}$ orthorhombic phase shown in Fig. 1. If we consider the perspective view of this structure, it appears that two successive layers of NiO_6 octahedra on either sides of a plane of oxygen vacancies are shifted between them by a vector $\frac{1}{2}\mathbf{a}$ (or $\frac{1}{2}\mathbf{c}$). Thus, if the plane structural faults correspond to planes of oxygen vacancies, a layer shifting must be observed along a [101] zone axis of orientation of this structure, i.e. the direction of observation of the high-resolution image in Fig. 5 (when assuming this structure). In order to verify it, we have superimposed a drawing derived from this structure to a part of this image (Fig. 5(b)). In this case, we have arbitrarily assumed that the white dots correspond to the columns of heavy atoms La and Ni (or more precisely Ni–O–Ni–O columns). Thus, on account of slight structural deformations, such a structural model fits quite well the high-resolution image.

Finally, as previously mentioned, the measured atomic La/Ni ratio in this layer by X-ray wavelength dispersive spectroscopy, (and also in all the layers deposited on other single crystal substrates) was found to be $La/Ni = 1.90 \pm 0.02$. Besides, by X-ray energy dispersive spectroscopy (XEDS) using an electron probe of 5 nm, the chemical composition of the layer was found to be homogeneous at this scale excepted for the intermediate layer shown in Fig. 4(b) which is very poor in lanthanum. In Section 4, we shall discuss of the relationship between the measured atomic La/Ni ratio and the density of plane structural faults.

3.2.2. *Analysis of the intermediate layer*

The intermediate layer of a thickness of about 4 nm was identified from high-resolution images of the layer–MgO interface oriented along the [100] and [110] zone axes of the MgO substrate and by X-ray energy dispersive spectroscopy using an electron probe of 5 nm (Fig. 6). From comparisons between the Fourier transforms of the image of this intermediate layer and those of the MgO substrate and $La_{1.9}NiO_x$ layer, it can be deduced that its structure is very similar to this of MgO. The Fourier transform pattern related to the $La_{1.9}NiO_x$ layer is similar to the electron diffraction pattern previously observed in Fig. 4(d) and to the Fourier transform shown in inset of Fig. 5(a). However, lines of diffuse scattering are not observed because the selected area for calculating this Fourier transform correspond to a small number of fringes. With respect to the cubic cell parameter of MgO (i.e. $a = 4.21$ Å), we have found that the cell parameter for this intermediate layer structure is slightly smaller (i.e. about 4.2 Å). Both

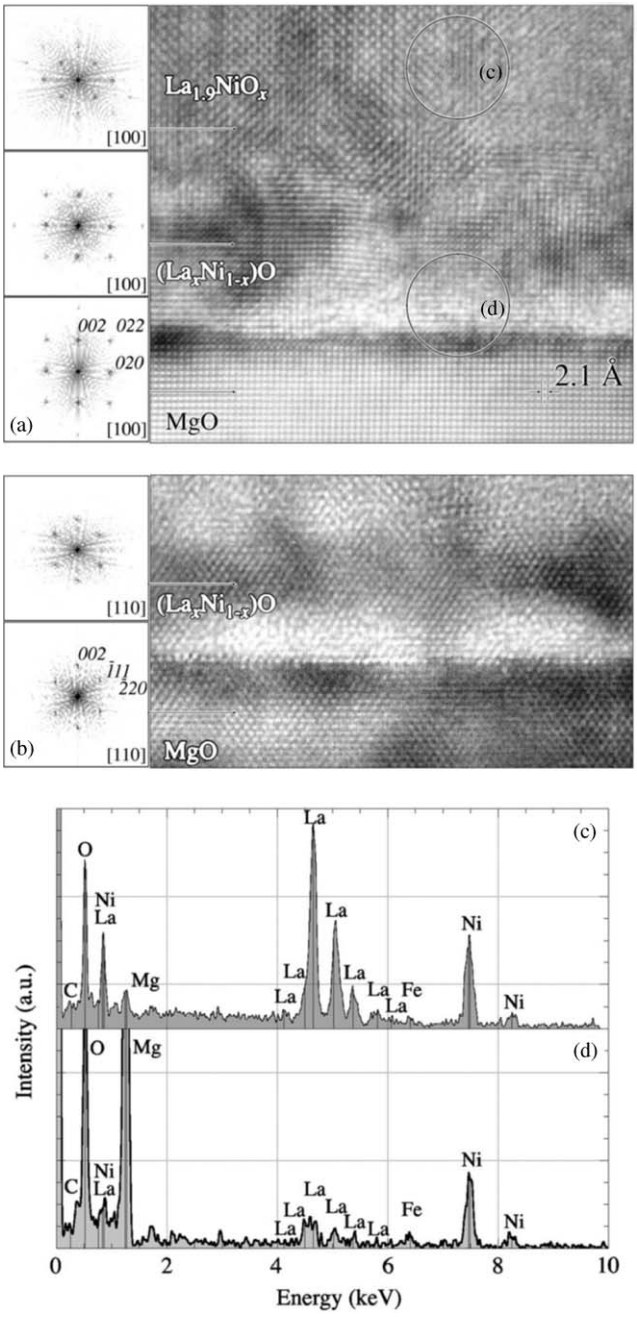

Fig. 6. High-resolution images of the layer–MgO interface oriented in (a) along the $[100]_{MgO}$ zone axis and in (b) along the $[110]_{MgO}$ zone axis. On the left-hand side of the figure, the Fourier transforms of different parts of these images are related to layers named $La_{1.9}NiO_x$ and $(La_xNi_{1-x})O$ and to the MgO substrate. Both spectra in the bottom part were obtained by X-ray energy dispersive spectroscopy from the encircled area (c) and (d) indicated in (a).

XEDS spectra shown in the bottom part of Fig. 6 correspond to analyses performed on the encircled area noted (c) and (d) in Fig. 6(a). These results are only qualitative. From their comparison, it appears that the intermediate layer, noted as $(La_xNi_{1-x})O$, does not contain La atoms (or just a very small proportion). There are very probably oxygen atoms but the oxygen peak results also from the MgO substrate. Let us note that the small peak of Fe observed on both spectra is probably due to an impurity contained in the metalorganic precursor $Ni(thd)_2$ and that the very small peak of carbon indicated that any carbon contamination has not occurred during these analyses.

On account of these observations one finds that this intermediate layer should correspond to NiO, which like MgO has a NaCl-type structure and a cell parameter of 4.18 Å. The solubility of La within the NiO phase is probably very low because La atoms are much bigger atoms than Ni atoms, (e.g. the cell parameter of the cubic LaO phase (also of NaCl type) is much larger ($a = 5.144$ Å)). Therefore, it seems that, in the first step of growth, a nucleation of NiO phase would be much easier than this of lanthanum nickelate oxide, probably because of a very small misfit of cell parameter between MgO and NiO phases (i.e. about 7×10^{-3}).

3.2.3. Pole figures

As TEM observations yield only a local information, the average crystallographic orientation relationships of layers on the different substrates (001)MgO, (001)$SrTiO_3$ and (001)$LaAlO_3$ were also studied by X-ray diffraction on a texture diffractometer. Different pole figures $\{220\}_L[001]_S$, $\{200\}_L[001]_S$ and $\{113\}_L[001]_S$ were determined as for instance, those shown in Fig. 7 for the layer deposited on (001)MgO. Such X-ray diffraction measurements were performed up to a ξ angle of 57.5° around the $[001]_{MgO}$ direction normal to the substrate. The selected reflections 220, 200 and 113 are those of the $La_2NiO_{4+\delta}$ tetragonal structure ($a = 5.46690$ Å, $c = 12.67804$ Å, space group $F4/mmm$), but might also correspond to reflections of a perovskite-like cubic structure, i.e. to 002, 110 and 112, respectively. For the MgO substrate, the orientation of its [100] and [001] axes as indicated in Fig. 7 were determined from a pole figure $\{220\}_{MgO}[001]_{MgO}$. From the $[110]_L$ stereographic projection of the $La_2NiO_{4+\delta}$ orthorhombic structure superimposed to experimental results, it appears that a four-fold symmetry is observed for both sets of measured 200 and 113 reflections, instead of a two-fold symmetry. Thus two orientations of the tetragonal cell could be considered. In this case, a (110) plane of the tetragonal cell would be parallel to the (001) surface of the MgO substrate and the **c**-axis of the tetragonal cell would either be parallel to $[100]_{MgO}$ or to $[010]_{MgO}$.

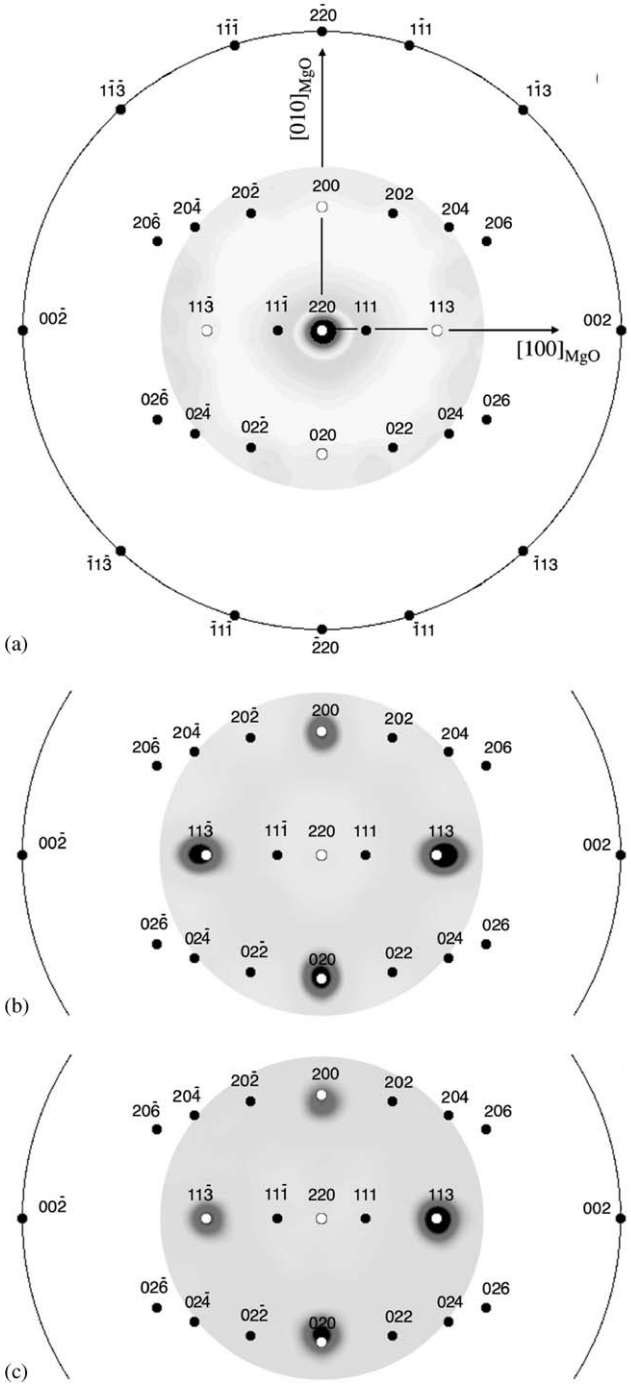

Fig. 7. Pole figures observed on the Lanthanum nickelate oxide layer deposited on the (001)MgO substrate. (a), (b) and (c) correspond, respectively, to $220_L[001]_{MgO}$, $200_L[001]_{MgO}$ and $113_L[001]_{MgO}$ poles figures. Measurements have been performed up a ξ angle of 57.5°. Crystallographic orientation relationships can either be deduced from the [110] stereographic projection of the $La_2NiO_{4+\delta}$ orthorhombic structure superimposed on the experimental results or by considering a perovskite-like cubic structure (see text).

However, on account of the previous TEM results, the crystallographic orientation relationships for a cubic structure of the layer are very simple: the ⟨100⟩ axes of both the layer and substrate are all parallel.

We have observed similar pole figures for the layers deposited on (001)$SrTiO_3$ and (001)$LaAlO_3$ substrates.

4. Discussion

In summary, depending on the substrate nature, two different structures of lanthanum nickelate oxide layers were obtained by injection MOCVD: dendritic layers of $La_2NiO_{4+\delta}$ tetragonal structure were observed on (001)Si substrate while a columnar microstructure of cubic structure, but with many (100) and (010) plane structural faults, was observed on a (001)MgO substrate. These structural faults were identified as being similar to the plane of oxygen vacancies of the $La_2NiO_{4+\delta}$ orthorhombic structure. One particularity of the lanthanum nickelate oxide layer on MgO substrate is to exhibit a very thin intermediate layer of cubic NiO phase on 4 nm thickness at the interface with the substrate. As the misfit of cell parameters between both MgO and NiO structures, of NaCl type, is very small (about 7×10^{-3}), it will be interesting to examine from further TEM observations if such a NiO layer exists or not on (001)$SrTiO_3$ and (001)$LaAlO_3$ substrates. We think that the difference of microstructure and structure between layers deposited either on (001)Si or on the other substrates could be due to the existence of an amorphous SiO_2 layer on (001)Si wafer which would impedes an epitaxial layer growth.

The La/Ni atomic ratio in all the deposited layers was found to be 1.90 ± 0.02 by X-ray wavelength dispersive spectroscopy, i.e. quite close to this of $La_2NiO_{4+\delta}$. A priori, a La/Ni ratio of 1.9 seems to be in contradiction with the idea that a layer of perovskite-like cubic structure should have a composition close $LaNiO_3$. An increase of the La/Ni ratio from 1 up to 1.9 must therefore be justified from a concentration of plane of oxygen vacancies similar to those of the $La_2NiO_{4+\delta}$ orthorhombic structure. From Fig. 5(a) and according to the structural model shown in Fig. 5(b), one can count along a horizontal direction (for instance the [100] of the perovskite structure) the number of $LaNiO_3$ cubic unit cell and the number of planes of oxygen vacancies (or plane structural faults). Since the $La_2NiO_{4+\delta}$ compound corresponds to a Ruddlesden–Popper phase $A_{n+1}B_nO_{3n+1}$ for $n = 1$ [21,22], it can be deduced that a plane of oxygen vacancies is equivalent to a stoechiometry AO (or $LaO_{1+\delta}$). Therefore, depending on the position of the horizontal line for counting, one finds 37 cubic unit cell and 15 or 16 planes of oxygen vacancies (plus about 1 plane of oxygen vacancies perpendicular to an orthogonal line). But as a similar number of crossing plane of oxygen vacancies of the $La_2NiO_{4+\delta}$ orthorhombic structure can be considered along the equivalent orthogonal axis [010], it results that the chemical formula of the layer writes (i.e. for 2×17 planes of oxygen vacancies and 37 cubic unit cells):

$$34LaO_{1+\delta} + 37LaNiO_3 = La_{71}Ni_{37}O_{145+34\delta} = La_{1.92}NiO_{3.92+0.92\delta}$$

which is in good agreement with the measured La/Ni ratio.

Finally, from first measurements of physical properties on the layers deposited on (001)$LaAlO_3$ and (001)MgO single crystal substrates, we have found a diamagnetic behavior with a small ferromagnetic component from $M(H)$ curves measured between 10 and 400 K by step of 10 K on a SQUID magnetometer. For instance, results of such magnetic measurements on a layer deposited on a (001)$LaAlO_3$ substrate are shown in Fig. 8(a). The diamagnetism can be attributed to the single crystal substrate and the ferromagnetic component which is still present at 400 K could probably correspond to the iron impurity as detected by TEM–XEDS (perhaps Fe_2O_3 or Fe_3O_4 oxides which the Curie temperature is in-between 575 and 600 °C).

Resistivity measurements were also performed on a layer deposited on (001)MgO substrate by a four-probe method between 30 and 300 K. As a result a

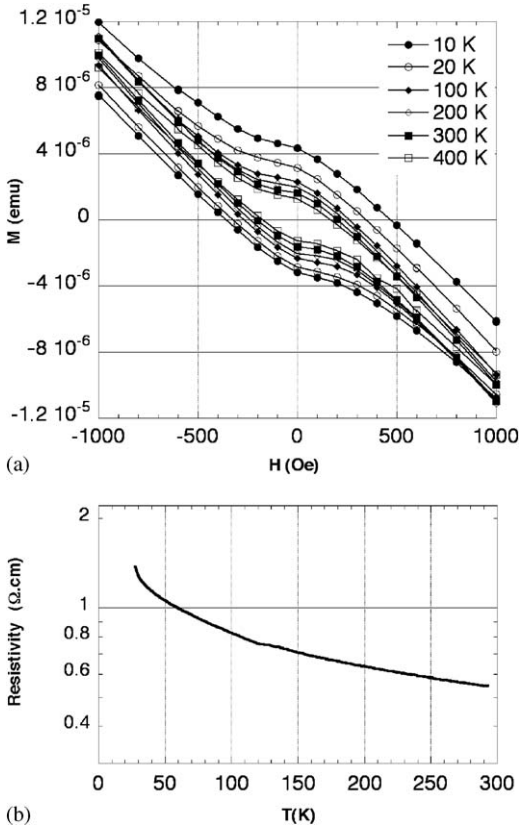

Fig. 8. (a) Magnetic measurements of $M(H)$ curves between 10 and 400 K performed on a lanthanum nickelate oxide layer deposited on (001)$LaAlO_3$ substrate, and (b) variation of the resistivity measured between 30 and 300 K on a layer deposited on a (001)MgO substrate (see text).

semi-conducting behavior is observed in a 20–300 K temperature range (Fig. 8(b)). At room temperature, the resistivity value is of 0.54 Ω cm and is coherent with results reported in the literature for $La_2NiO_{4+\delta}$ compounds [23–25]. However, down to 30 K, the behavior of the resistivity is best described by a variable-range hopping mechanism which is coherent with the observed disorder of plane structural faults [26]. Further measurements are in progress on layers grown on single crystalline substrates in order to study the anisotropy of transport properties.

Acknowledgments

This work was supported by the European Community (CERMOX contract No G5RD-CT2000-00351).

References

[1] J.G. Bednorz, K.A. Muller, Z. Phys. B 64 (1986) 189.
[2] D.J. Buttrey, H.R. Harrison, J.M. Honig, R.R. Schartman, J. Solid State Chem. 54 (1984) 407.
[3] D.C. Zhu, X.Y. Xu, S.J. Feng, W. Liu, C.S. Chen, Catalysis Today 82 (2003) 151.
[4] M.J. Sayagues, M. Vallet-Regi, J.L. Hutchison, J.M. Gonzales-Calbet, J. Solid State Chem. 125 (1996) 133.
[5] J.D. Jorgensen, B. Dabrowski, Shiyou Pei, D.R. Richerds, D.G. Hinks, Phys. Rev. B 40 (1989) 2187.
[6] Z. Hiroi, T. Obata, M. Takano, Y. Bando, Phys. Rev. B 41 (1990) 11665.
[7] J.M. Bassat, P. Odier, A. Villesuzanne, C. Marin, M. Pouchard, Solid State Ionics 167 (2004) 341.
[8] N. Poirot, P. Odier, P. Simon, F. Gervais, Solid State Sci. 5 (2003) 735.
[9] J. Rodriguez-Carjaval, M.T. Fernández-Daz, J.L. Martnez, J. Phys.: Condens. Matter 3 (1991) 3215.
[10] D.J. Buttrey, P. Ganguly, J.M. Honig, C.N.R. Rao, R.R. Schartman, G.N. Subbanna, J. Solid State Chem. 74 (1988) 233.
[11] H.J.M. Bouvmeester, A.J. Burgraaf, in: A.J. Burgraaf, L. Cot (Eds.), Fundamentals of Inorganic Membrane Science and Technology, Membrane Science and Technology Series, vol. 4, Elsevier, Amsterdam, Lausanne, New York, Oxford, Shannon, Tokyo, 1996, p. 435.
[12] B.CH. Steele, in: U. Bossel (Ed.), Proceedings of the First European SOFC Forum, European Fuel Cell Forum (Oberrohrdorf), vol. 1, 1994, p. 375.
[13] S. Shinomori, M. Kawasaki, Y. Tokura, Applied Phys. Lett. 80 (2002) 574.
[14] S. Pignard, H. Vincent, J.P. Sénateur, P.H. Giauque, Thin Solid Films 347 (1999) 161.
[15] J.P. Sénateur, R. Madar, F. Weiss, O. Thomas, A. Abrutis, French patent FR 2707671 (1993), European patent EP 730671 (1994), US patent US 945162 (1999).
[16] V.V. Kharton, A.P. Viskup, A.V. Kovalevsky, E.N. Naumovich, F.M.B. Marques, Solid State Ionics 143 (2001) 337.
[17] A. Sharma, Z.-G. Ban, S.P. Alpay, J.V. Mantese, J. Appl. Phys. 95 (2004) 3618.
[18] D. de Ligny, P. Richet, Phys. Rev. B 53 (1996) 3013.
[19] Z.-G. Ban, S.P. Alpay, J. Appl. Phys. 91 (2002) 9288.
[20] Z.-G. Ban, S.P. Alpay, J. Appl. Phys. 93 (2003) 504.
[21] S.N. Ruddlesden, P. Popper, Acta Crystallogr. 10 (1957) 538.
[22] S.N. Ruddlesden, P. Popper, Acta Crystallogr. 11 (1958) 54.
[23] C.N.R. Rao, D.J. Duttrey, N. Otsuka, P. Ganguly, H.R. Harrison, C.J. Sandberg, J.M. Honig, J. Solid State Chem. 51 (1984) 266.
[24] K. Ishikawa, W. Shibata, K. Watanabe, T. Isonaga, M. Hashimoto, Y. Suzuki, J. Solid State Chem. 131 (1997) 275.
[25] G. Wu, J.J. Neumeier, Phys. Rev. B 67 (2003) 125116.
[26] C. Ang, J.R. Jurado, Z. Yu, M.T. Colomer, J.R. Frade, J.L. Baptista, Phys. Rev. B 57 (1998) 11858.